INTERACTION OF THE SOLAR WIND WITH VENUS

H. S. Bridge, A. J. Lazarus, and G. L. Siscoe
Massachusetts Institute of Technology
Cambridge, Massachusetts

and

R. E. Hartle, K. W. Ogilvie, and J. D. Scudder
NASA/Goddard Space Flight Center
Greenbelt, Maryland

and

C. M. Yeates
Jet Propulsion Laboratory
Pasadena, California

ABSTRACT

Two topics related to the interaction of the solar wind with Venus are considered. First, a short review of the experimental evidence with particular attention to plasma measurements carried out on Mariner-5 and Mariner-10 is given. Secondly, the results of some recent theoretical work on the interaction of the solar wind with the ionosphere of Venus are summarized.

INTRODUCTION

The plasma interaction region at Venus (charged particles and magnetic fields) has been explored by several spacecraft. The discussion in this paper is limited to results obtained by Venera-4 (Gringauz et al., 1968, 1970), Mariner-5 (Bridge et al., 1967), Venera-6 (Gringauz et al., 1970), and Mariner-10. The Venera-4 and Mariner-5 encounters occurred respectively on October 18 and 19, 1967; Venera-6 on May 17, 1969; and Mariner-10 on February 5, 1974. It is, of course, well known that large changes in plasma properties and in the magnitude and direction of the magnetic field were observed by all of these spacecraft in the vicinity of Venus. These changes in the field and plasma seem very similar to those observed in passing through the bow shock of the Earth, and the observations were interpreted by the Venera-4 and Mariner-5 experimenters in terms of a similar detached bow shock at Venus. However, the bow shock at Earth results from the interaction between the solar wind and the geomagnetic field and the distance to the shock is typically about 14 R_E. In contrast, the shock at Venus is observed much closer to the planet. This result leads to the conclusion that the intrinsic magnetic field of Venus is very small compared to that of the Earth. Estimates of the possible dipole field of Venus based on the above experiments correspond to a

magnetic moment between 10^{-3} and 10^{-4} that of Earth. The absence of a planetary magnetic field and the results of the Mariner-5 radio propagation experiment concerning the Venus ionosphere led the Mariner-5 plasma and magnetic field investigators to conclude that the solar wind interacted directly with the ionosphere of Venus and produced a bow shock which was similar to that observed at Earth, but which was very close to the planet.

Prior to the Venera-4 and Mariner-5 missions, extensive calculations had been carried out for the plasma flow around the geomagnetic field using the methods of classical fluid dynamics (Spreiter et al., 1966). In these models, the ram pressure of the solar wind is balanced by the magnetic pressure and there is no transfer of momentum or energy across the magnetopause. The theoretical predictions for the positions of the bow shock and magnetopause agreed very well with observations for distances not far downstream from the Earth. These theoretical results were used together with experimental data about the shape of the Earth's bow shock to interpret the early observations at Venus. In 1970, Spreiter et al. (1970) carried out an extensive series of calculations for the plasma flow around Venus. The method and assumptions were similar to those used previously for the Earth, but the ram pressure of the wind was balanced by the static gas pressure of the ionosphere. As in the previous work, it was assumed that there was no interaction at the boundary between the plasma flow and the obstacle, that is, that the ionopause was a tangential discontinuity.

EXPERIMENTAL RESULTS

A comparison of the experimental results with this theory is shown in figure 1. In this representation, it is assumed that the interaction is axially symmetric about the Venus-Sun line which forms the x-axis. Data points along the various trajectories have been rotated about this line into a common plane. The positions of the bow wave and ionopause shown in the figure have been calculated under the assumption of flow along the x-axis, and have used preliminary values* of solar-wind speed and density (410 km s^{-1} and 11 cm^{-3}) observed by Mariner-10. This implies a ram pressure during the Mariner-10 encounter somewhat greater than that observed during the Mariner-5 encounter. The dotted curves are drawn for a ratio of ionospheric scale height to obstacle radius, $H/r_0 = 0.25$. With the appropriate change of scale, they correspond quite closely to a typical Mach 5 shock observed at Earth. The solid curves are for the case $H/r_0 = 0.01$.

Although the experimental data agree qualitatively with the theory, it is very difficult to make a quantitative comparison given the limited and incomplete data set. Some of the problems are as follows:

- The location of the boundaries changes in response to changes in the upstream conditions in the solar wind. The velocity of the boundary is in general much greater than the spacecraft velocity and multiple crossings are often observed.

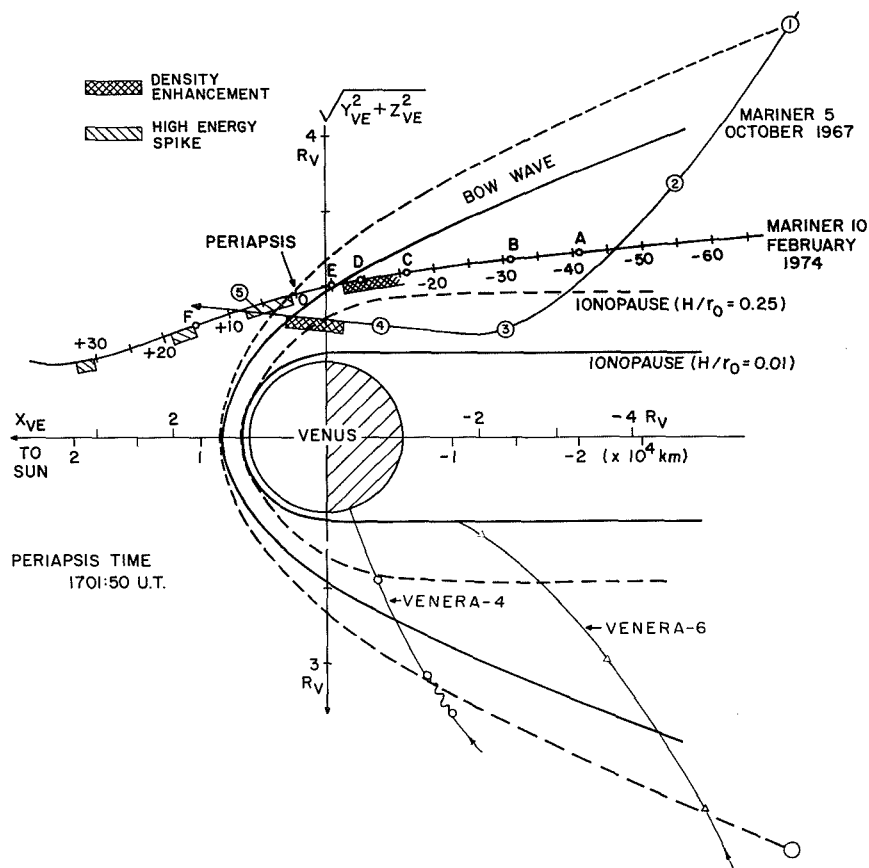*Final values are not available at this time.

Figure 1. The Venera-4, Mariner-5, Venera-6, and Mariner-10 trajectories in a plane containing the Venus-Sun line. The planet and two predictions of fluid theory for the case of flow along the Venus-Sun line are also shown. The letters refer to events along the track of Mariner-10, and the circled numbers refer to events along the track of Mariner-5.

- The upstream conditions are not known at the times measurements were made in the interaction region so it is difficult to know whether variations observed near the planet result from variations in solar-wind conditions or whether they are caused by the interaction.

- The orientation of the magnetic field strongly influences conditions at the boundary.

In general, the observed shock transitions are sharper and more clearly defined on the dusk* side where the magnetic field tends to be parallel to the shock boundary, and diffuse or pulsating on the dawn side when the field is usually more nearly perpendicular to the boundary (Greenstadt, 1972).

---

*In the following discussion, the terms dawn and dusk are used in the conventional sense of observations at Earth, that is, the retrograde rotation of Venus is ignored.

Keeping these points in mind, the following comments about the data shown in figure 1 can be made.

Venera-4, Mariner-5, and Venera-6 approached Venus from the evening side. On all three spacecraft, characteristic changes in the plasma and magnetic-field data were observed on the inbound trajectory which showed clearly that the spacecraft had passed from the undisturbed solar wind into a disturbed region of transitional flow similar to the magnetosheath of Earth. The shock boundary was crossed downstream from the terminator at an angle to the Sun line of about 114° for Venera-4, 138° for Mariner-5, and 135° for Venera-6. The outbound shock crossing of Mariner-5 was on the dawn side upstream from the terminator at an angle of $\sim$75°. On Venera-4 the planar ion traps measured the plasma flux above 50 V every 14 s down to a few hundred kilometers above the surface. No information about the plasma flow speed or temperature was obtained but since the ion flux dropped to the background level at about 1.5 R_V, the spacecraft clearly passed completely through the pseudo-magnetosheath into a region where the flow velocities and ion densities were very low. The Venera-4 planar ion traps could measure ion densities in a stationary plasma near the planet for ion densities greater than $\sim$10^3 cm^{-3}. No such inner zone was observed. The Venera-6 mission carried instruments similar to those of Venera-4 but continuous data were not transmitted close to the planet. A clear shock crossing was recorded at $\sim$6.9 R_V.

The Mariner-5 plasma probe measured the energy-per-charge spectrum of the plasma ions over a 40-V to 9.4-kV range in 32 logarithmically-spaced contiguous windows. The flux sensitivity was $\sim$2 X 10^6 cm^{-2} s^{-1} and during the encounter phase of the mission, a complete measurement was made every 5.04 min. During the cruise phase of the mission, measurements of the flow direction were carried out. However, no directional measurements were made during the encounter phase. Mariner-5 also carried a helium vector magnetometer which made four unequally-spaced measurements of the magnetic field every 12.6 s; in the original publication the field data are 50-s averages. Significant changes in the plasma and field observed by Mariner-5 are shown by the circled figures on the trajectory in figure 1. At point (1), the plasma density and temperature increased markedly and the flow speed decreased slightly. The absolute magnitude of the field increased by nearly a factor of two and the fluctuations in the field increased significantly. Between (1) and (2) for a time of about one hour, the plasma speed decreased slightly from the initial post-shock values of 580 km s^{-1} and 5.5 cm^{-3}. At point (2) the value of B decreased suddenly, the magnitude of the fluctuations increased, and the plasma density and velocity began a smooth decrease which reached minimum values of $\sim$0.1 cm^{-3} and 300 km s^{-1} near event (3) and returned to higher values near event (4). Between events (4) and (5), there was a broad density spike which lasted 10 to 15 min and a coincident broad maximum in the magnitude of the magnetic field. During this interval, the velocity was relatively constant and slightly less than the values measured before the inbound shock crossing and after the outbound crossing. The outbound shock crossing was taken rather arbitrarily to correspond with point (5). Given the increase in our knowledge since 1967 and the benefit of hindsight, several comments can be made about the Mariner-5 results and various interpretations which have been advanced since that time.

66

Mariner-5 Results

First of all, it is obvious that the plasma measurements were strongly affected by time aliasing in regions where the plasma properties changed rapidly (that is, a time of 5 min or a distance of ~3000 km). The effect is especially severe because, during the 32-step energy scan, the energy did not increase monotonically with time. Instead, the 32 contiguous windows were divided into four sets of eight noncontiguous windows and in each of the four sets, the eight windows were uniformly spaced across the energy/charge range of the instrument. Thus, in each eight-step scan, measurements were made over nearly the complete energy/charge interval (40 V to 9.4 kV) but the total coverage in energy/charge space was only 25 percent. Thus, if the ion spectrum is broad compared to the window width, it is possible to increase the time resolution of the Mariner-5 plasma measurements by a factor of four.

We have re-examined the Mariner-5 plasma data and find that significant additional information can be obtained from the individual scans, that is, it is possible to increase the time resolution by about a factor of four. A semiquantitative presentation of the results is given in figure 2. In this figure, an individual energy/charge scan is represented by the horizontal velocity scale for protons from roughly 110 to 1000 km/s. The vertical bars indicate the currents observed in individual velocity channels, and the height of the bar is proportional to the logarithm of the flux density in an individual channel. Successive scans are spaced uniformly along the ordinate and are separated by ~1.25 min. The time in minutes relative to encounter is shown along the ordinate and the data set extends from about an hour before encounter until about one-half hour after encounter. The circled numbers along the ordinate correspond to the numbered features in the original publication (see figure 3).

There are at least two important features which were not recognized in the presentation of the original Mariner-5 results which are apparent from an inspection of the data shown in figure 2. Starting at about E-47.5 and ending at E-7.5, the fluxes observed in individual channels decrease in amplitude, shift to lower velocities, and vary greatly in amplitude from one scan to the next. At E-25, E-15, and E-10, the observed flux is below the sensitivity of the instrument. This time interval begins ~10 min before event (3) and ends near event (2). Inspection of the trajectory plots (see figure 4) shows that, during this time interval, the Mariner-5 spacecraft was close to the geometrical shadow of Venus (closest approach to the geometrical shadow was at E-22) and, hence, close to a possible cavity in the plasma wake. The disappearance of the plasma flux at the times noted above is consistent with the hypothesis that the spacecraft crossed a boundary between the region of transitional flow behind the shock and a cavity which could contain a stationary plasma not detectable by the Mariner-5 plasma probe.

The second noteworthy feature is that, on the outgoing trajectory, the bow shock is crossed at E+15. This is clearly evident in the proton spectra shown in figure 2 and represents a significant change from the original value of E+20. The consequences of this revision are considered in a later section of this report.
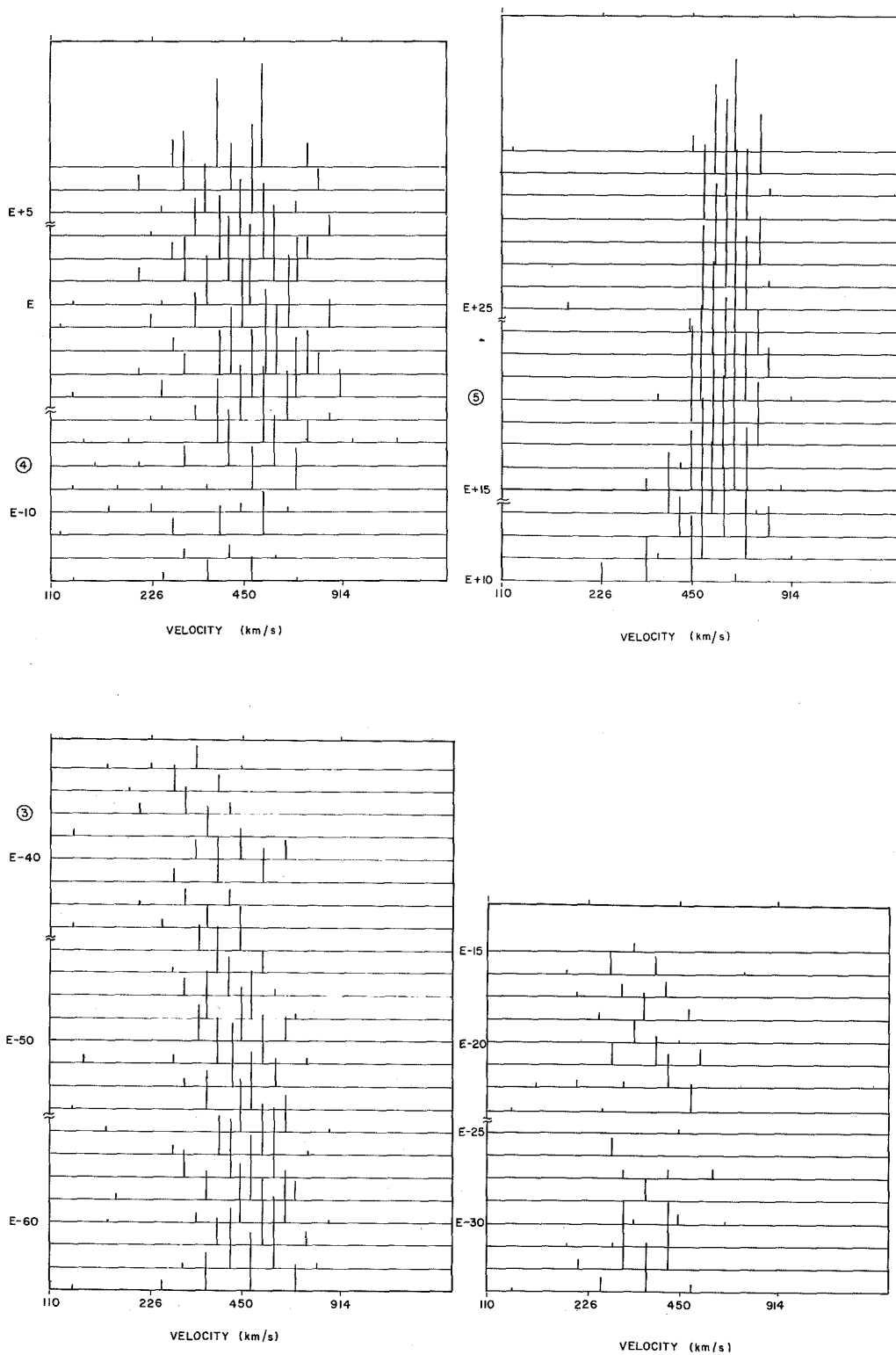
Figure 2. High-time resolution data of Mariner-5 during Venus encounter (see text).
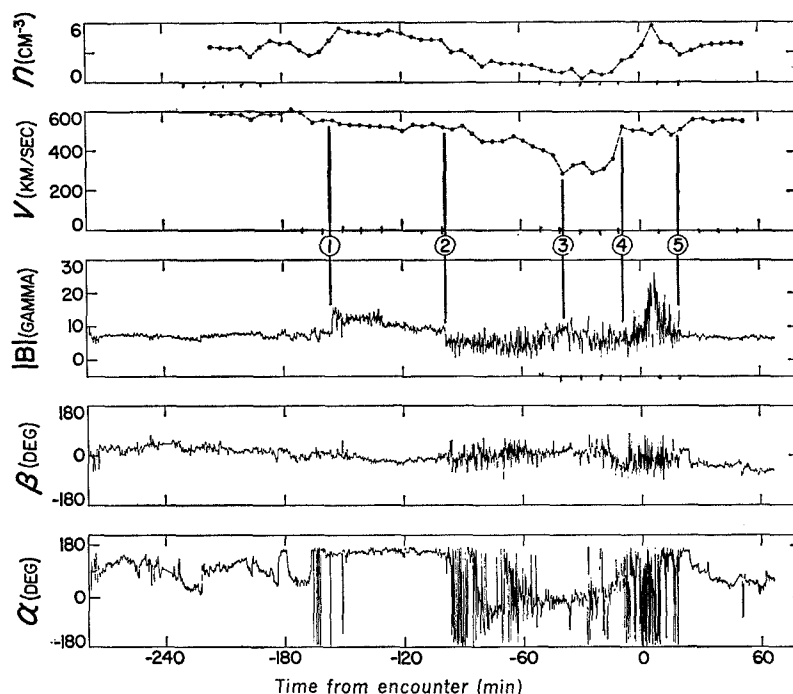
Figure 3. Mariner-5 plasma and magnetic field data near Venus. Time indicated as zero corresponds to closest approach. Vertical lines and circled numbers denote features of special interest discussed in the text.

Mariner-10 Results

Preliminary reports of plasma and magnetic-field measurements carried out at Venus by Mariner-10 have been published (Bridge et al., 1974; Ness et al., 1974). Although final results from these experiments are not yet available, the current state of analysis and interpretation can be summarized as follows.

The Mariner-10 plasma measurements were obtained with an electrostatic analyzer mounted on a scan platform. The analyzer measured electrons in the energy range from 13 to 715 eV in 15 logarithmically-spaced windows of width $\Delta E/E = 6.6$ percent. Because of an instrument failure, no measurements of ions were made. The scan axis was approximately perpendicular to the ecliptic plane and the fan shaped field of view subtended ~7° in the scan plane and 27° in a plane parallel to the scan axis. The total angular scan was 120° and the analyzer always viewed the antisolar hemisphere. During Venus encounter, an angular scan was made every 30 s and a complete energy scan every 6 s. The fluxgate magnetometer used on Mariner-10 made a measurement of the vector field every 40 ms. However, the data discussed here have been averaged over a longer interval.
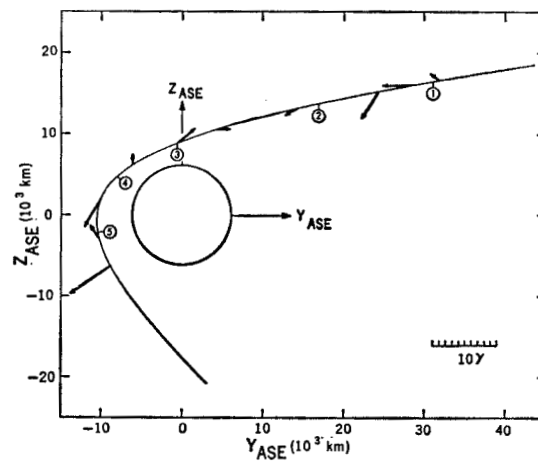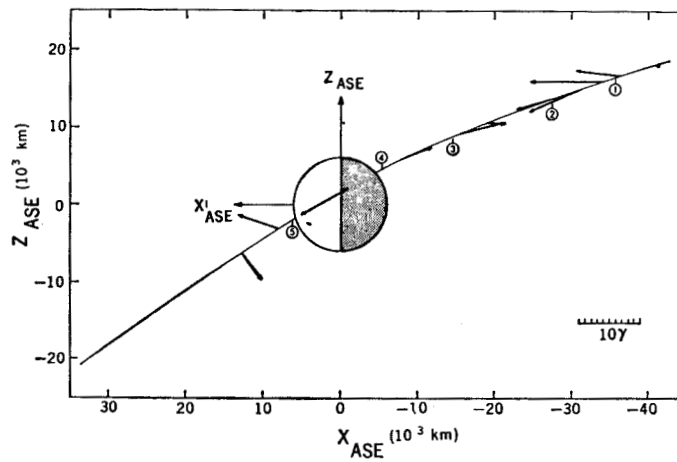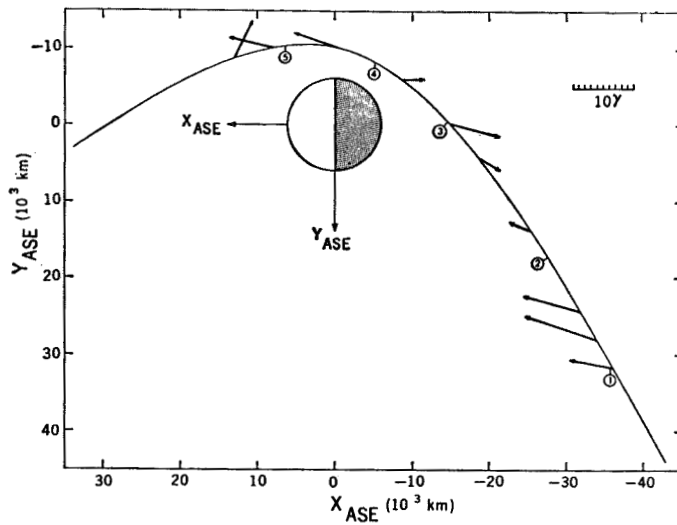
69

Figure 4. Mariner-5 trajectory and magnetic-field vectors. The three panels contain aphrodiocentric-solar-ecliptic projections of the trajectory and of the measured field at specific points.

Figure 5 shows the plasma and magnetic-field data obtained during a period of 2.5 hours during the Venus encounter. From top to bottom, the first four data fields show:

- 84-s averages of the field magnitude,

- The angle, ϕ, of the field in the ecliptic plane relative to the Sun-spacecraft line,

- The inclination angle, θ, relative to the ecliptic plane,
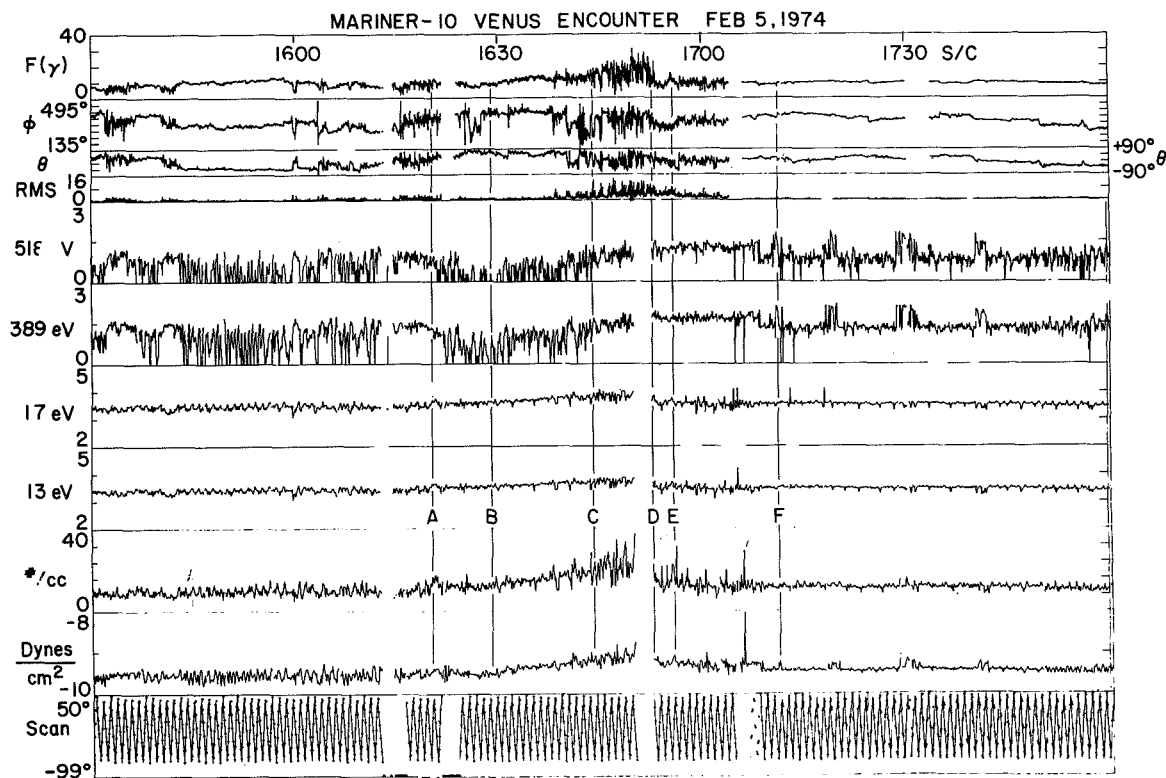
- The RMS deviation of the field.

Figure 5. Plasma and magnetic-field data obtained during the Mariner-10 Venus encounter.

The next four data fields show the plasma flux recorded in two low-energy and in two high-energy channels:

- In the 13-eV channel,

- In the 17-V channel,

- In the 389-V channel,

- In the 539-V channel.

The bottom three data fields show:

- The electron number density,

- The pressure,

- The angle of the scan platform.

Six features of particular interest are identified by letters A through F in figure 5. The general features of the observations are as follows.

As the planet is approached, the density generally increases, reaches a maximum about 10 min before periapsis, and then drops rapidly to half its maximum value. Throughout the encounter period, the density never decreases substantially below the upstream solar-wind value of ~10 electrons/cm^3. Superimposed upon this broad density feature are many large-amplitude, short-period variations which suggest the presence of turbulent flow. The electron distribution functions always decrease monotonically toward higher energies; low-energy flux channels usually control the densities. In the region of the density maximum, the fluxes in the high-energy channels are a factor of ~100 larger than those usually observed in the solar wind. After the density decrease, there are several discontinuous density increases, up to the last density spike, labeled event E in figure 5.

Characteristic features are seen in the data from the high-energy channels. At the beginning of the gradual rise in density, the flux at high energy begins to decrease rather rapidly (event A). After 9 min, the high-energy flux reaches a minimum (event B) and then rises to the predecrease value after 15 min (event C). Point C occurs 8 min before the density decrease (event D). At its minimum, the flux in the high-energy channel is about one-fifth as much as its value in the upstream solar wind, and this feature is general in channels above ~100 eV. The flux in this energetic electron bite-out interval is highly modulated at the scan frequency, which indicates that the flux is very directional. Several smaller decreases of short duration occurred in high-energy channels before event A.

The magnetic field data shown in figure 5 exhibit several regions which have distinctly different magnetic signatures. The large-amplitude fluctuations observed between 16:38:30 and 16:53:30 UT were interpreted in the original Mariner-10 publication as "being associated with approach and immediate proximity to the bow shock." The bow-shock crossing was taken to be at 16:51:30 UT. Upstream from the bow shock, the data show smaller-amplitude higher-frequency fluctuations which persist until about 17:06 UT. The plasma experimenters took the bow-shock crossing to be just after the density maximum at about 16:55 or just before event E shown in figure 5. From the Mariner-10 data and from the previous results of Venera-4, Mariner-5, and Venera-6, there seems little doubt that the original interpretation of the plasma and field data in terms of a standing bow shock at Venus is correct.

Mariner-5 and -10 Data Comparisons

It should be kept in mind that the Mariner-5 and -10 data concerning the bow shock should be compared with shock crossings on the dawn side of the Earth where the interplanetary magnetic field tends to be perpendicular to the bow-shock surface. For this case, the bow shock (the so-called pulsating shock) is thick and diffuse when defined by changes in the magnetic field or plasma electron data, but thin and sharp in terms of the plasma protons. In contrast, the bow shock observed on the evening side where the field tends to be parallel to the shock is sharp and well-defined in terms of the magnetic field, the plasma electrons, and the plasma protons. Thus, the magnetometer data of Mariner-5 and the magnetometer and plasma electron data of Mariner-10 showed diffuse bow-shock crossings at Venus which are completely consistent with similar data obtained at Earth. The results at the first encounter of Mariner-10 with Mercury agree well with this picture. In this case, the incoming and outgoing shock crossings were somewhat downstream from the terminator but it is noteworthy that the evening-side crossing was sharp, whereas the dawn-side crossing was remarkably similar to that seen at Venus.

In comparing the data with a particular model, there are some important consequences which arise from the difficulty of defining the exact position of the shock. Given the Mariner-5 or -10 data, a reasonable uncertainty might be four or five minutes which corresponds to a distance along the trajectory of about 3000 km. At Earth, this kind of uncertainty is negligible compared to the scale size of the obstacle and the experimental data can be compared directly with the predictions of a fluid model. At Venus or Mercury, however, this uncertainty in the boundary location is comparable to the size of the obstacle. Thus, a detailed comparison of the experimental results with theory may not be extremely fruitful. For example, a change in H/r_0 from 0.25 to 0.01 would shift the predicted shock boundary location along the Mariner-10 trajectory by about 3000 km. However, if one assumes that the change in temperature of the plasma protons is the relevant parameter in defining the bow-shock position and if one uses the revised Mariner-5 plasma proton data discussed above, then the observed shock crossing is close to the predicted location shown in figure 1 for $H/r_0 = 0.01$. This conclusion is not changed if one allows the wind direction to be 4° from the west during the Mariner-5 encounter. (This was the observed direction just after encounter.)

Anisotropies Observed

The anisotropies observed in the fluxes at energies above 100 eV when the spacecraft was between events A and C on the trajectory should now be discussed. This depletion of the high-energy electron flux is not observed in the terrestrial magnetosheath and represents a unique characteristic of the Venus observations which we attribute to a direct interaction between the solar wind and the Venus atmosphere. This is almost certainly the case since the observed decreases in the fluxes of high-energy electrons correspond primarily to a loss of electrons moving along magnetic flux tubes which connect to the dayside of the planet.

We suggest that the electron flux is depleted by scattering in the neutral atmosphere as the electrons move along magnetic field lines which pass through the atmosphere.

A recent interpretation of the topside electron density distribution of Venus from the Mariner-10 radio occultation experiment suggests that the solar wind penetrates to an altitude of at least 250 km and that solar-wind scavenging takes place at this level (Bauer and Hartle, 1974). In this model the dominant neutral constituent in the 200- to 250-km altitude range is atomic oxygen. Oxygen has a peak cross section $\sigma \cong 1.5 \times 10^{-16}$ cm^2 for electron impact ionization at 100 eV. Furthermore, the cross section remains high for electron energies up to 800 eV and is relatively low below $\sim$80 eV. This is just the energy dependence which is required to explain the electron flux depletion. According to Bauer and Hartle (1974), the oxygen density, N, may be as large as 5×10^8 cm^{-3} at 250 km. Thus, the mean free path is

$$\lambda = \frac{1}{\sigma N} = \frac{1}{10^{-16}\ 5 \times 10^8} = 2 \times 10^7 \text{ cm @ 100 eV}$$

and has increased to

$$\lambda = 3 \times 10^7 \text{ cm @ 800 eV}$$

Since the mean free path is less than the planet radius $R \cong 6 \times 10^8$ cm at ionopause altitudes, it is quite likely that the magnetosheath electrons interact with the atmosphere strongly enough to explain the observed flux depletion.

The proposed ionization process produces additional electrons in the 0- to 100-eV energy range. The corresponding density increase is

$$\Delta N_e \cong \sigma\ N_e^1\ N\ 2 \times R \cong 10^{-16} \times 10^{-1} \times 5 \times 10^8\ 2 \times 6 \times 10^8 = 6 \text{ cm}^{-3}$$

where N_e^1 is the electron density for electron energies $>$80 eV and $2 \times R$ is the distance traveled by the electrons. This calculated value of ΔN_e represents a 50-percent increase in the electron density above the magnetosheath background and is in good agreement with the increased fluxes in the low-energy channels observed in the depletion region.

INTERACTION WITH THE ATMOSPHERE AND IONOSPHERE

In this section a brief summary of some recent results of Harel and Siscoe* is given. Their calculations illustrate two possible modifications of the solar-wind flow which might arise from its interaction with the atmosphere and ionosphere. The first result concerns the maximum modifications of the flow parameters which could be expected because of the pickup of atmospheric ions by the wind.

---

*Harel, M. and G. L. Siscoe, Stagnation Streamline Calculations, private communication, 1975.

The neutral atmosphere extends above the ionopause and can interact with the solar wind as it becomes ionized through the processes of photoionization, charge exchange, and collisional ionization. The interaction can be studied theoretically by the addition of appropriate source and loss terms in the equations for the conservation of mass, momentum, and energy in the solar wind (see, for example, Holzer, 1972). The form of the additional terms depends on the assumed nature of the interaction mechanism and two extreme cases can be considered. In one, the new ions are assumed to become thermalized with respect to the solar-wind ions in a short time compared to the time during which the flow parameters change appreciably (in effect, instant thermalization). In the other extreme, the new ions do not thermalize, but interact with the solar wind through the solar-wind motional electric field and magnetic field which transfer momentum and energy from the solar-wind ions to the atmospheric ions.

The results of a calculation in which the first assumption was made are given here. The first case is instructive by itself since it gives an upper limit for the magnitude of the solar-wind modification that can be expected from the atmospheric effect.

The calculation uses the technique of expanding the hydrodynamic equations in a Taylor series in the radial distance away from the stagnation streamline in the region between the bow shock and the stagnation point. Terms up to second order are retained, and boundary conditions imposed by the strong shock jump relations are used to integrate the coefficients of the expansion along the stagnation streamline from the shock to the stagnation point.

Three existing models of the Venus upper atmosphere were used. One assumes helium (He) dominant with a density of 10^7 cm^{-3} at the ionopause, one assumes deuterium (D) dominant with an ionopause density of 10^5 cm^{-3}, and the third assumes hydrogen (H) dominant with an ionopause density of 10^4 cm^{-3}. Scale heights based on a temperature of 675 K were used (He, 175 km; D, 350 km; H, 700 km). These calculations were performed before the Mariner-10 results were available and, consequently, some of these input data are appreciably different from the best current estimates. However, the calculations are intended to illustrate the qualitative results of some extreme assumptions and are not intended to represent the situation at Venus in a quantitative sense. For comparison, a calculation with no atmosphere was performed. The no-atmosphere and helium-atmosphere results are shown in figures 6 and 7. In these figures, T is the temperature, U is the coefficient of the radial velocity (away from the stagnation streamline), D is mass density, V is velocity along the stagnation streamline, and N is the mass density of the atmospheric ions. For the purpose of this presentation, the absolute values of the quantities are not important (except N), but only the relative comparison between the two figures. The shock is on the left margin, and ionopause is coincident with the stagnation point where V = 0, and is at 0.83 in units of distance normalized to the radius of curvature of the bow shock at its nose.

A large effect near the ionopause due to the atmosphere is evident. The temperature decreases because of the assumed thermalization of the ions. The mass density increases because of ion pickup and also because the divergence of the flow away from the stagnation
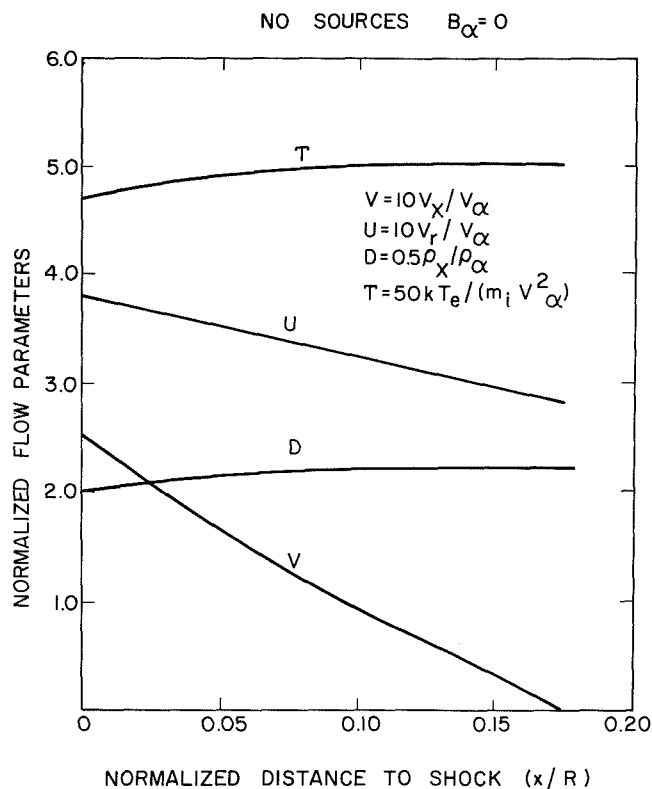
Figure 6. Stagnation streamline calculation for no atmosphere. Upstream values of the flow parameters are indicated by the subscript α.

region is reduced as indicated by the reduction in U. There is little effect on V. The atmospheric ion density increases to a maximum at the ionopause. In absolute values at the stagnation point, 16 percent of the ions are atmospheric helium ions. For a typical solar-wind ion number density of 5 H^+ cm^{-3}, the absolute value of He^+ at the stagnation point is 6 cm^{-3}. As the material diverges away from the stagnation region and moves along the boundary layer, more atmospheric ions will be picked up. Thus, the relative He^+ density in the detached boundary layer will be greater than 16 percent.

A calculation similar to that described above for the effect of the neutral atmosphere was performed with source terms appropriate to energy loss to the electron component by heat conduction through the ionopause to the ionosphere. In this calculation the effect of atmospheric neutrals was not included. The ion and electron components were treated separately and coupled by the requirement of charge neutrality. Because of the greater mobility of the electrons, only heat loss by electrons was included. The ions were assumed to be adiabatic. An important unknown parameter in the calculation is the electron heat conduction coefficient. A large range of values was used, and all gave the same qualitative behavior of the plasma parameters. Figure 8 gives results for the case with coefficient based on an effective collision frequency equal to the ion acoustic wave frequency ($\sim$100 Hz). The curve for V is

HELIUM ATMOSPHERE ($n_o = 10^7 cm^{-3}$) $B_\alpha = 0$
SOURCES: PHOTOIONIZATION AND CHARGE-EXCHANGE

$V = 10 V_x / V_\alpha$
$U = 10 V_r / V_\alpha$
$D = 0.5 \rho_x / \rho_\alpha$
$T = 50 k T_e / (m_i V^2_\alpha)$

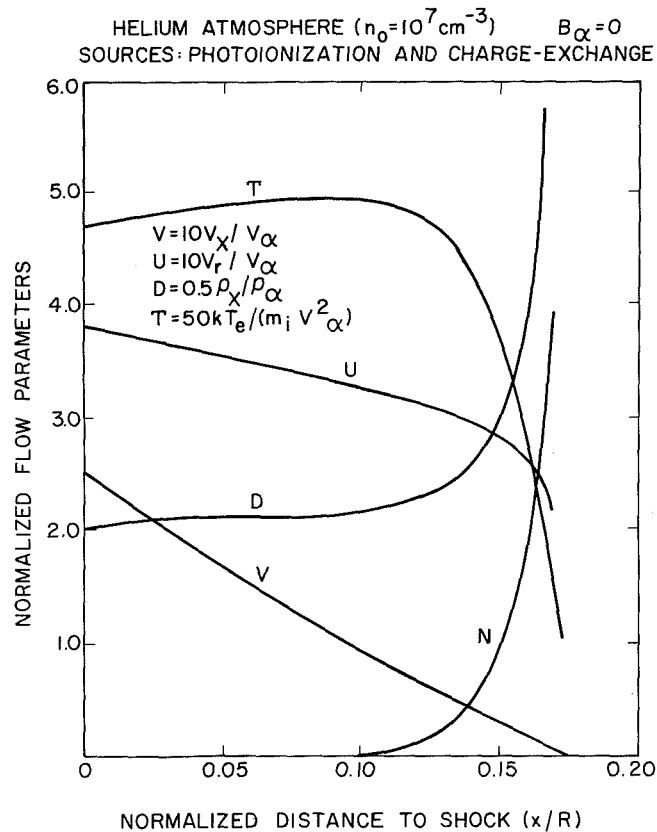NORMALIZED FLOW PARAMETERS

NORMALIZED DISTANCE TO SHOCK (x/R)

Figure 7. Stagnation streamline calculation for helium atmosphere. N is the mass density of the atmospheric ions normalized to the solar-wind ion density.

very similar to the no-interaction case (figure 7). The electron temperature goes to zero at the ionopause. This is a boundary condition on the solution since the temperature must fit smoothly onto the ionospheric electron temperature, which is essentially zero compared to the solar-wind value. The density goes up at the stagnation point compared to the no-interaction case. The increased density is expected since the proton pressure (nkT_p) must increase to compensate for the missing electron pressure (nkT_e). The curve labeled (T) shows the electron heat flux along the stagnation line. The calculation shows that at the ionopause the heat flux is approximately 20 percent of the upstream, incident kinetic energy flux ($1/2 \ \rho V^3$). The results also show that the ionospheric effect being investigated here extends well into the ionosheath for the assumed conduction coefficient. In figure 9, the case of zero heat conduction and B perpendicular to incoming V is shown. Note the increase in magnetic pressure and corresponding decrease in particle density near the stagnation point.
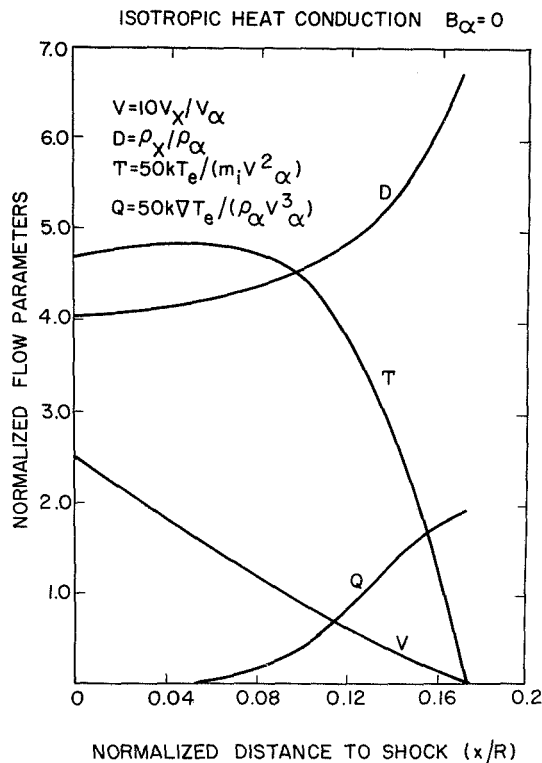
ISOTROPIC HEAT CONDUCTION $B_\alpha = 0$

NORMALIZED FLOW PARAMETERS

$V = 10 V_X / V_\alpha$
$D = \rho_X / \rho_\alpha$
$T = 50 k T_e / (m_i V^2_\alpha)$
$Q = 50 k \nabla T_e / (\rho_\alpha V^3_\alpha)$

NORMALIZED DISTANCE TO SHOCK (x/R)

Figure 8. Stagnation streamline calculation showing the effect of electron heat conduction into the ionosphere.

NO HEAT CONDUCTION $B \perp V$

NORMALIZED FLOW PARAMETERS

$V = 10 V_X / V_\alpha$
$U = 10 V_r / V_\alpha$
$D = \rho_X / \rho_\alpha$
$T = 50 k T_e / (m_i V^2_\alpha)$
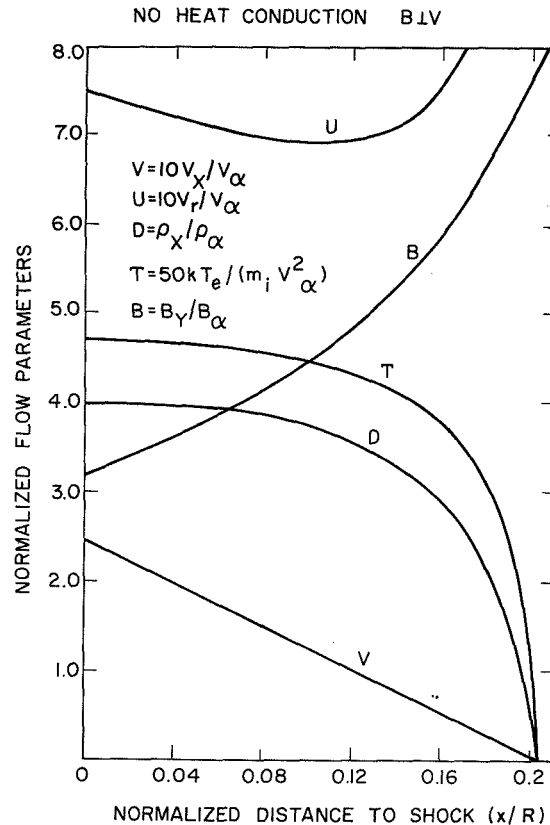$B = B_Y / B_\alpha$

NORMALIZED DISTANCE TO SHOCK (x/R)

Figure 9. Stagnation streamline calculation for the case B perpendicular to V.

REFERENCES

Bauer, S. J. and R. E. Hartle, 1974, "Venus Atmosphere: An Interpretation of Mariner 10 Observations," *Geophys. Res. Lett.*, **1**(1), pp. 7-9.

Bridge, H. S., A. J. Lazarus, C. W. Snyder, E. J. Smith, L. Davis, Jr., P. J. Coleman, Jr., and D. E. Jones, 1967, "Mariner V: Plasma and Magnetic Fields Observed Near Venus," *Science*, **158**, pp. 1659-1663.

Bridge, H. S., A. J. Lazarus, J. D. Scudder, K. W. Ogilvie, R. E. Hartle, J. R. Asbridge, S. J. Bame, W. C. Feldman, and G. L. Siscoe, 1974, "Observations of Venus Encounter by the Plasma Science Experiment on Mariner 10," *Science*, **183**, pp. 1293-1296.

Greenstadt, E. W., 1972, *J. Geophys. Res.*, **77**, p. 1729.

Gringauz, K. I., V. V. Bezrukikh, L. S. Musatov, and T. K. Breus, 1968, "Plasma Measurements Conducted in the Neighborhood of Venus by the Space Apparatus "Venera-4," " *Kossmicheskiye Issledovaniya*, **6**(3), pp. 411-419.

Gringauz, K. I., V. V. Bezrukikh, G. I. Volkov, L. S. Musatov, and T. K. Breus, 1970, "Interplanetary Plasma Disturbances Near Venus Determined from "Venera-4" and "Venera-6" Data," *Kossmicheskiye Issledovaniya*, 8(3), pp. 431-436.

Holzer, T. E., 1972, "Interaction of the Solar Wind with the Neutral Component of the Interstellar Gas," *J. Geophys. Res.*, 77, pp. 5407-5431.

Ness, N. F., L. W. Behannon, R. F. Lepping, Y. C. Whang, and K. H. Schatten, 1974, "Magnetic Field Observations Near Venus: Preliminary Results from Mariner 10," *Science*, 183, pp. 1301-1306.

Spreiter, J. R., A. L. Summers, and A. Y. Alksne, 1966, "Hydromagnetic Flow Around the Magnetosphere," *Planet. Space Sci.*, 14, pp. 223-253.

Spreiter, J. R., A. L. Summers, and A. W. Rizzi, 1970, "Solar Wind Flow Past Nonmagnetic Planets—Venus and Mars," *Planet. Space Sci.*, 18, pp. 1281-1299.

QUESTIONS

Bridge/Gringauz: What is the thickness of the bow-shock front according to the Mariner-10 data?

Bridge: The bow-shock transition observed on Mariner-10 by the magnetometer or the high-energy electrons (greater than 100 eV) is diffuse and the thickness quoted depends on an arbitrary definition. A reasonable estimate would be 1500 km. On the other hand, the bow shock observed by Mariner-5 in the proton data occurred in a time interval of less than one minute which corresponds to less than a 600-km thickness. The location of the Mariner-5 shock defined by the change in magnetic field is uncertain by at least 2000 to 3000 km. That is, there is no sharp magnitude discontinuity which coincides with the change in the proton spectrum.